Publishing House
AKAPIT

COMPUTER METHODS IN MATERIALS SCIENCE

Informatyka w Technologii Materiałów

Vol. 11, 2011, No. 2

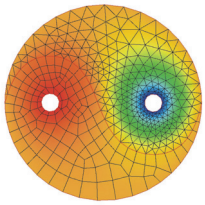

SIMULATION OF THERMO-MECHANICAL PROCESSES DURING HOT FORGING AND PREDICTION OF MECHANICAL PROPERTIES OF PRODUCTS

VALERIY PIDVYSOTS'KYY, JAROSŁAW OPARA, ANDRZEJ WROŻYNA, WŁADYSŁAW ZALECKI, ROMAN KUZIAK*

Instytut Metalurgii Żelaza im. St. Staszica, K. Miarki Street 12-14, 44-100 Gliwice, Poland
**Corresponding author: rkuziak@imz.gliwice.pl*

Abstract

This paper presents the results of physical and numerical simulation of forging followed by controlled-cooling processes. Rheological, microstructural and phase transition models for the simulation were developed using Gleeble 3800 and DIL 805A/D. All models were implemented into the FE code. The microstructure and mechanical properties of final products were predicted. Results of simulation were compared with mechanical properties of actual forging.

Key words: numerical simulation, rheological model, microstructural model, phase transition model, mechanical properties

1. INTRODUCTION

The final properties of forgings used in the automobile industry are traditionally achieved by the application of heat treating operation. To reduce the production costs, microalloyed steel grades were developed in late 80-ies, giving required properties in the as forged state. The microalloyng elements used for the austenite microstructure evolution control and precipitation strenghtening include Ti, Nb and V. These grades are currently being in use for the production of forged parts, which are utilised in the automobile industry. An interesting way of enhancing the strength properties of forgings, which will be analysed in this paper, is the application of accelerated cooling directly after forging. As a rule, accelerated cooling increases the degree of austenite undercooling leading to the refinement of ferrite – pearlite microstructure. It may be applied either to conventional C-Mn or to microalloyed grades.

2. MATERIAL AND EXPERIMENTAL PROCEDURE

Production technology of forging shown in figure 1 was the subject of this investigation. The aim of the process was to achieve the required properties by using in the production conventional C45 steel grade, combined with accelerated cooling after forging. Chemical composition of C45 steel is given in table 1.

Steel bar having the dimensions 90x90x137 mm was induction heated to 1220°C and forged in three strokes, followed by accelerated cooling in cooling device with a set of fans. Cooling start temperatures in the trial varied in the range 800÷1000°C. To assess the austenite grain size, water cooling directly after forging was applied. After cooling down to ambient temperature, the samples were taken for mechanical properties measurement and quantitative structure characterization (pearlite and ferrite volume fractions,

 ISSN 1641-8581

prior austenite grain size, ferrite grain size and pearlite interlamellar spacing). The location of the area for measurements is marked in figure 1. Prior austenite grain boundaries and pearlite – ferrite microstructure of the forging is shown in figure 2.

Table 1. *Chemical composition of C45 steel grade.*

C	Mn	Si	Cr	Mo	Ti	V	Nb	Cu
0.46	0.56	0.23	0.03	0.008	<0.001	<0.004	<0.004	0.07

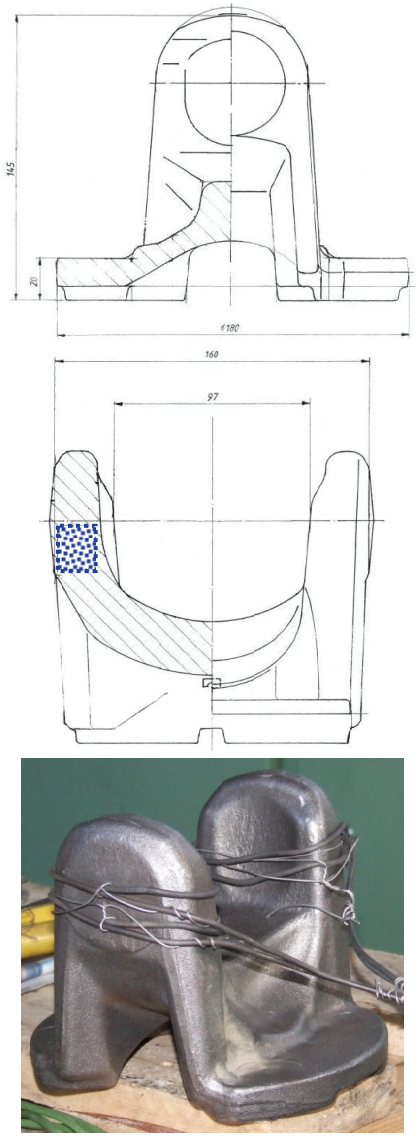

Fig. 1. *Experimental forging of Cardan joint (microstructure and hardness were examined in dotted area).*

Quantitative measurements of the microstructure in the selected area showed that the average prior austenite grains size (equivalent diameter) was 61÷76 μm, ferrite volume fraction in pearlitic-ferritic microstructure amounts to 13÷19 pct, average ferrite grain size was 9 μm and pearlite interlamellar spacing 220 nm. Yield strength and ultimate strength were equal to 548 MPa and 790 MPa, respectively. Hardness of forging was 228 HV10.

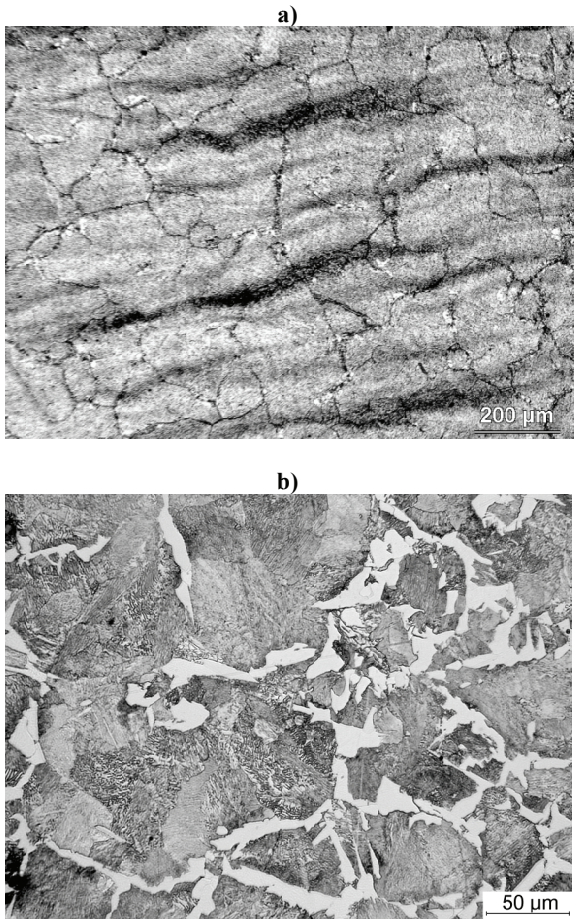

Fig. 2. *Prior austenite grain boundaries – (a) and pearlite-ferrite microstructure – (b) in the area of forging marked in figure 1.*

3. PLASTOMETRIC TESTS

Plastometric tests were conducted to develop the rheological and microstructure evolution model. Tests were conducted using Gleeble 3800 simulator. Cylindrical samples ∅10×12mm were deformed in the simulator in order to determine the following material characteristics:

– Rheological model.
– Kinetics of dynamic, metadynamic and static recrystallization.
– Grain growth kinetics following recrystallization.

In the investigation, stress relaxation technique was used to assess the kinetics of metadynamic and static recrystallization. Water quenching was applied after deformation for the sake of grain size assessment.

Phase transitions in C45 steel were investigated by means of DIL 805A/D dilatometer. Two types of specimens were used: tube ∅4×∅2×10mm for CCT diagrams and cylinder ∅4×10mm for DCCT (Deformation Continuous Cooling) diagrams.

4. RESULTS

4.1. Microstructure evolution and rheological model

In first stage of investigation grain growth model during heating was developed. The kinetics of grain growth is represented by the following equations:

$$D^{8.29} = D_0^{8.29} + 2.0608 \cdot 10^{42} \exp\left(-\frac{740\,323.77}{RT}\right) t \qquad T \le 1423\ K$$

$$D^{7.429} = D_0^{7.429} + 1.5096 \cdot 10^{28} \exp\left(-\frac{450\,169.06}{RT}\right) t \qquad T > 1423\ K \tag{1}$$

Next, the rheological and dynamic recrystallization models were formulated on the basis of Davenport-Sellars (D-S) model (Davenport et al., 1999; Kowalski, 2000) and in the project modified dynamic recrystallization model in which austenite grain size in equation for dynamically recrystallized volume fraction, X_{dyn}, was developed:

$$\sigma_p = \sigma_0 + (\sigma_{sse} - \sigma_0)\left[1 - \exp\left(-\frac{\varepsilon}{\varepsilon_r}\right)\right]^{\frac{1}{2}} - (\sigma_{sse} - \sigma_{ss}) X_{dyn}$$

$$\sigma_0 = \frac{1}{\alpha_0} \sinh^{-1}\left(\frac{Z}{A_0}\right)^{\frac{1}{n_0}},$$

$$\sigma_{ss} = \frac{1}{\alpha_{ss}} \sinh^{-1}\left(\frac{Z}{A_{ss}}\right)^{\frac{1}{n_{ss}}},$$

$$\sigma_{sse} = \frac{1}{\alpha_{sse}} \sinh^{-1}\left(\frac{Z}{A_{sse}}\right)^{\frac{1}{n_{sse}}}$$

$$Z = \dot{\varepsilon} \exp\left(\frac{Q_{def}}{RT}\right), \qquad \varepsilon_r = \frac{1}{3.23}\left[q_1 + q_2 (\sigma_{sse})^2\right],$$

$$X_{dyn} = 1 - \exp\left(p_8 \left(\frac{\varepsilon - \varepsilon_c}{\varepsilon_s - \varepsilon_c}\right)^{p_9}\right),$$

$$\varepsilon_c = p_1 \varepsilon_m, \qquad \varepsilon_s = p_2 D_0^{\,p_3} Z^{p_4},$$

$$\varepsilon_m = p_5 D_0^{\,p_6} Z^{p_7} \tag{2}$$

Optimal parameters for modified D-S model are given in table 2. Examples of fitting model D-S and modified D-S model (for the coefficients given in table 2) with true stress – strain curves (after using inverse analysis) are given in figure 3.

The dynamically recrystallized grain size was calculated with the following equation:

$$d_{rec}^{dyn} = 1168.58 Z^{-0.1245} \tag{4}$$

To predict the static and metadynamic recrystallization kinetics, the Avrami's equation was used. Equations (5) and (7) described static and metadynamic recrystallization kinetics respectively. The austenite grain size upon the static and metadynamic recrystallization completion is calculated with equations (6) and (8) respectively.

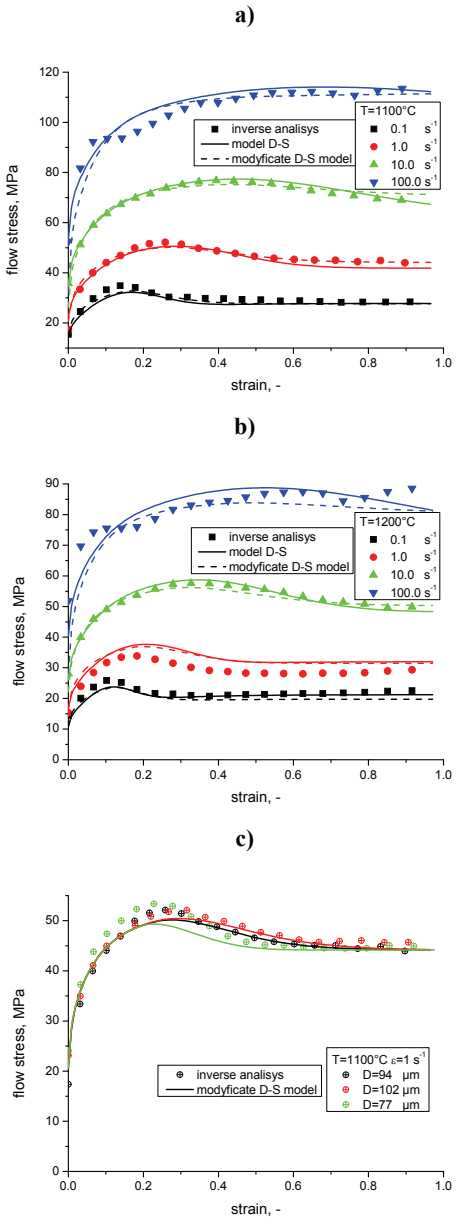

Fig. 3. Comparison of the results of calculations stress-strain curves using D-S and modified D-S model with experimental results for 1100°C – (a), 1200°C – (b) and influence of grain size on flow stress – (c).

Table 2. *Optimal parameters for modified D-S model.*

Rheology – σ_0			Q_{def}
A_0	n_0	α_0	
$1.2363 \cdot 10^{7}$	0.13262	3.0375	280 203.64

Rheology – hardening and dynamic recovery				
$A_{ss(e)}$	$n_{ss(e)}$	$\alpha_{ss(e)}$	q_1	q_2
$1.66110 \cdot 10^{16}$	6.98599	$5.41445 \cdot 10^{-03}$	0.6913	$6.66096 \cdot 10^{-06}$

Rheology – dynamic recrystallization		
A_{ss}	n_{ss}	α_{ss}
$1.59723 \cdot 10^{18}$	6.6929	$3.29208 \cdot 10^{-03}$

p_1	p_2	p_3	p_4
0.88	$5.26712 \cdot 10^{-06}$	1.47596	0.19823

p_5	p_6	p_7	p_8	p_9
$6.89021 \cdot 10^{-05}$	0.79948	0.18753	-1.66863	1.62773

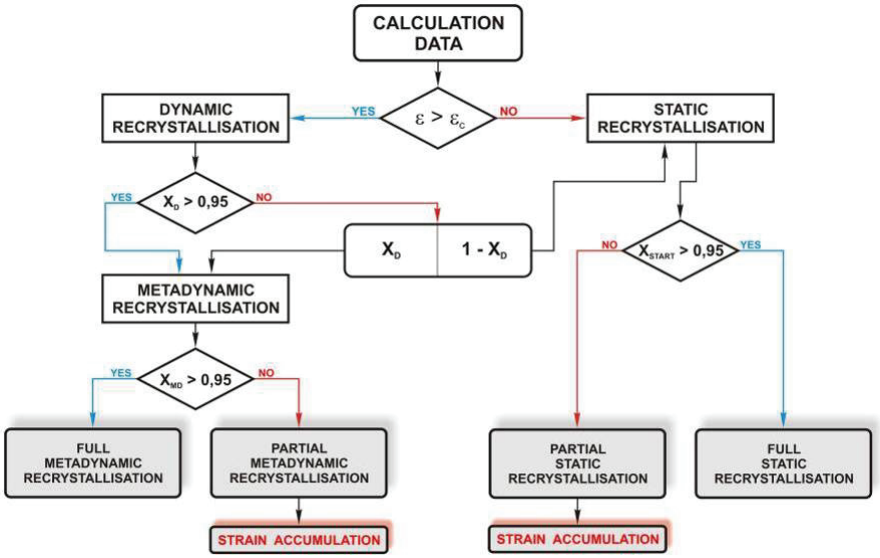

Fig. 4. *Algorithm for the simulation of austenite microstructure evolution during hot deformation.*

$$X_{st} = 1 - \exp\left(-\ln(2) \left[\frac{t}{t_{0.5}^{st}} \right]^{0.86} \right),$$

$$t_{0.5}^{st} = 2.199 \cdot 10^{-16} \varepsilon^{-1.0784} \dot{\varepsilon}^{-0.4204} D_0^{3.5972} \exp\left(\frac{186000}{RT} \right) \quad (5)$$

$$D_{rec}^{st} = 28.713 \varepsilon^{-0.3} \dot{\varepsilon}^{-0.0796} D_0^{0.1746} \exp\left(-\frac{6445.95}{RT} \right) \quad (6)$$

$$X_{md} = 1 - \exp\left(-\ln(2) \left[\frac{t}{t_{0.5}^{md}} \right]^{0.93} \right),$$

$$t_{0.5}^{md} = 4.1665 \cdot 10^{-4} Z^{-0.5088} \exp\left(\frac{210898.07}{RT} \right) \quad (7)$$

$$d_{rec}^{md} = 3341.33 Z^{-0.2146} \quad (8)$$

The following equations were used for the calculation of grain growth kinetics after the recrystallization completion:

$$D^5 = D_0^5 + 2.5837 \cdot 10^{19} \exp\left(-\frac{302085.87}{RT} \right) t \quad (8)$$

A general schematic diagram of the numerical algorithm for the simulation of austenite microstructure evolution during the rolling process is shown in figure 4.

The calculation of the effective strain after initiation of the recrystallization process in a material was performed using the following relation:

$$\varepsilon_r^i = \left(\varepsilon_r^{i-1} + \varepsilon^i \right) \left(1 - X_{st}^i \right) \quad (9)$$

where i is current pass deformation, ε_r^{i-1} is cumulative strain after preceding deformations ($i = 1$; $\varepsilon_r^{i-1} =$

0), ε^i is current deformation, X_{st}^i is volume fraction of recrystallized material.

The developed model was implemented into Forge 3D commercial code for the simulation of experimental steel forging.

4.2. Phase transformation model

For modeling of the phase transformations, built-in phase transformation model of the Forge commercial code was applied. Also, our own model was developed for the experimental steel using the approached originally formulated by Kirkaldy and modified by Victor Li et al., 1998; Saunders et al. using the CCT diagram of experimental steel (figure 5). However, the implementation of this model into Forge program faced many difficulties and is currently under way.

$$\sigma_y = f_\alpha\left[77.7 + 59.5Mn + 9.1D_\alpha^{-0.5}\right] + \left[145.5 + 3.5S_0^{-0.5}\right] + 478N^{0.5} + 1200P$$

$$\sigma_s = f_\alpha\left[20 + 2440N^{0.5} + 18.5D_\alpha\right] + \left[750(1 - f_\alpha)\right] + \left[\left(1 - f_\alpha^{0.5}\right)\left(3S_0^{-0.5}\right)\right] + 92.5Si \quad (10)$$

Microstructural parameters of equation (10) are calculated with following equations:

$$D_\alpha = \left[7.05 - 8.37C - 1.63Mn + 8.5V - 20N\right]D_\gamma^{0.2}C_r^{-0.25}$$

$$S_0 = 0.13 + 1.027C - 1.93C^2 - 0.1107Mn + 0.0305C_r^{-0.52} \quad (11)$$

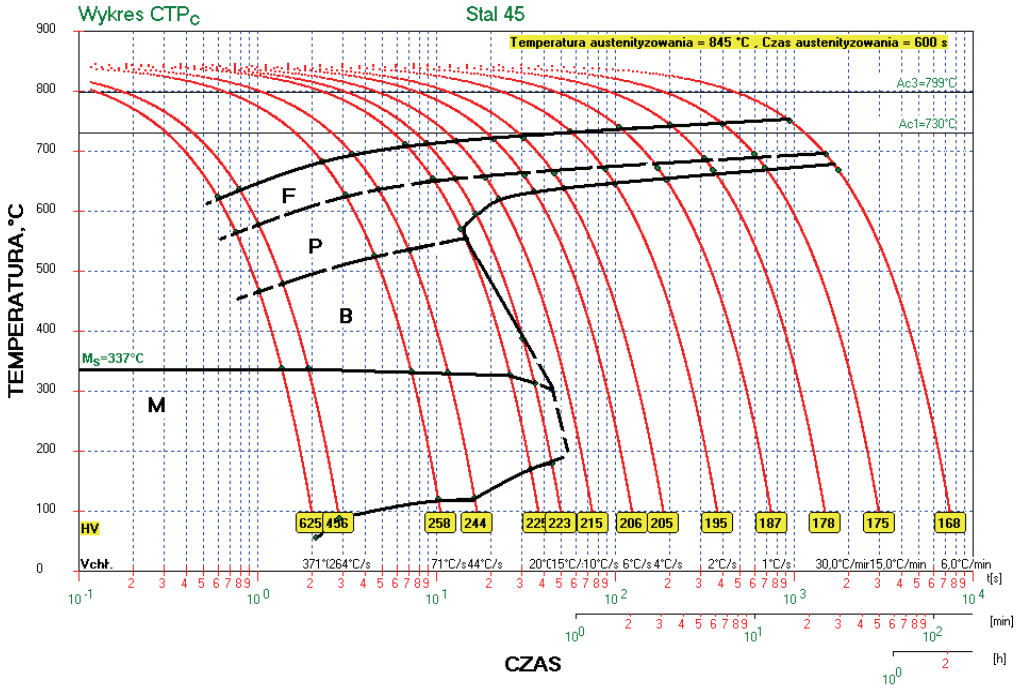

Fig. 5. CCT diagram of C45 steel.

4.3. Mechanical properties

The prediction of yield strength and ultimate tensile strength in the final product was conducted using empirical model accounting for chemical composition, grain size D_α, interlamellar spacing in cementite S_0, cooling rate C_γ and volume fraction of phases. The model was originally developed by Kuziak R. et al., 1997:

4.3. Results of the simulation

At the beginning of the process modelling, three strokes conducted during forging were simulated. Evolution of microstructure during deformations is presented in figure 6. A flash was cut off after deformation and the forging was subjected to accelerated cooling with the set of fans. The time period between end of forging and beginning of accelerated cooling lasts around 20 s. Although flash cutting off does not influence microstructure, its simulation makes mesh

at the edge of forging much more complicated. Therefore, this process has been replaced by 20 s period of slow cooling applied to the forging without flash (figure 6e). Temperature distribution after forging and before accelerated cooling is presented in figures 7. The maximum value of the residual strain after first stroke is equal to 0.1. The highest increment of residual strain was revealed after second stoke (figure 8).

Results of accelerated cooling after phase transformations completion are presented in figure 9.

Comparing simulation and microstructural measurement results good conformity was found in prior austenite grain size (65µm predicted versus 68.5µm obtained in measurement). The model predicts higher ferrite volume (21%) comparing with measurements (av. 16%). This discrepancy is acceptable. Ferrite grain size (3.8 µm predicted versus 9 µm obtained in measurement) and pearlite interlamellar spacing (220 nm versus 147 nm) calculated are lower then measured. However, predicted mechanical properties are in good agreement with measurements (σ_y^p = 525 Mpa and σ_s^p = 785 MPa versus σ_y^m = 548 MPa, σ_s^m = 790 MPa). The prediction of hardness is not correct (calculated 275HV vs measured 228HV), because the commercial software does not take into account parameters of pearlite structure, e.g: interlamellar spacing.

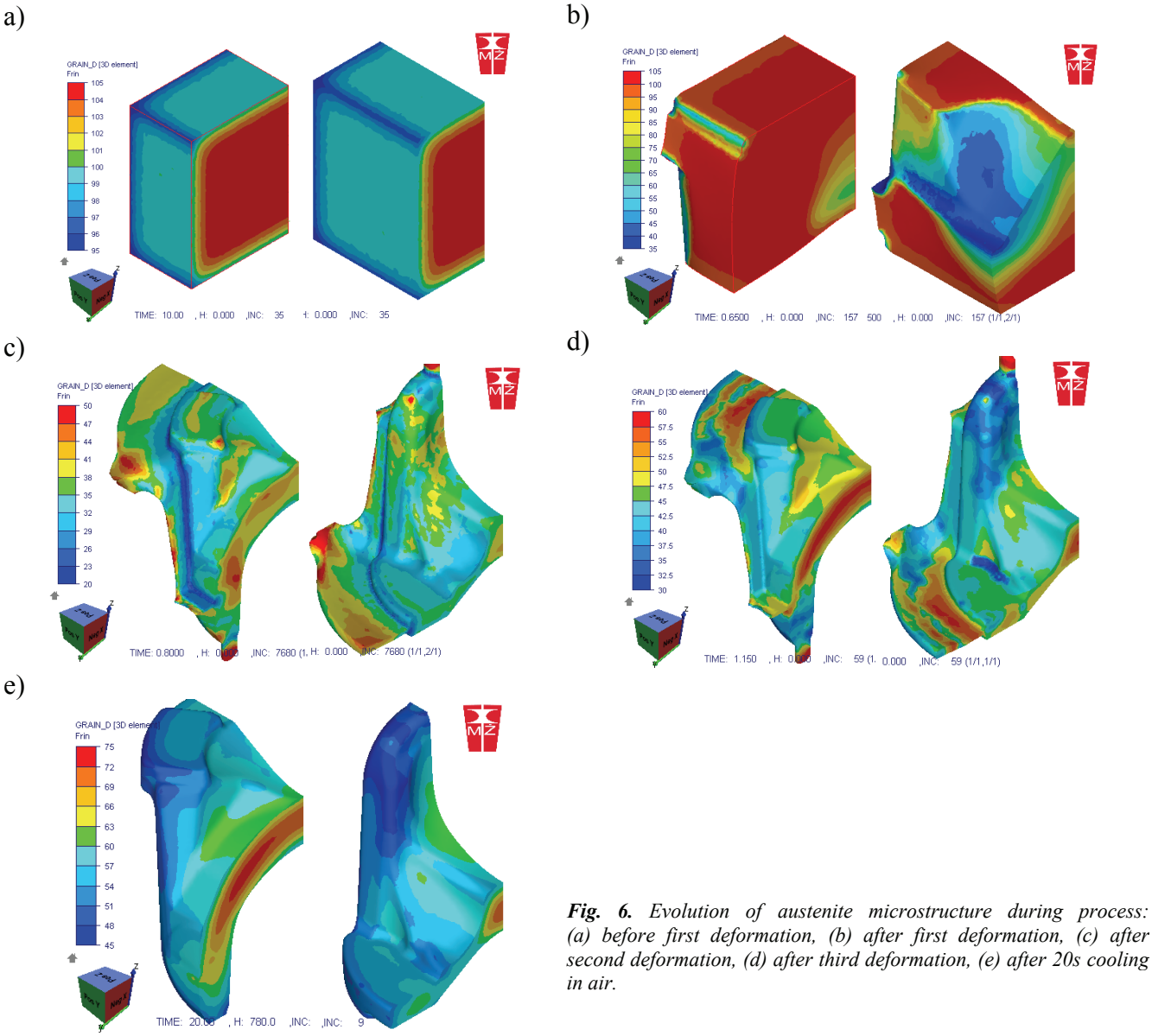

Fig. 6. *Evolution of austenite microstructure during process: (a) before first deformation, (b) after first deformation, (c) after second deformation, (d) after third deformation, (e) after 20s cooling in air.*

In the second stage of simulation, the evolution of temperature in the forging subjected to accelerated cooling was calculated. In real process, the cooling is carried out in a duct under assembly of three fans, where the first one is the most efficient. In work (Kuziak et al., 2010) it was determined that heat exchange coefficient changes from 200 W/(m^{2}K) in the first phase of cooling to 50 W/(m^{2}K) at the end. These conditions were represented in the simulation.

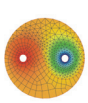

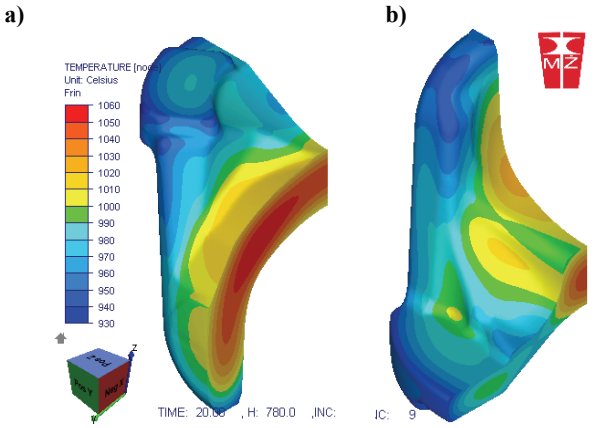

Fig. 7. *Distribution of temperature after forging (a) and directly before accelerated cooling (b).*

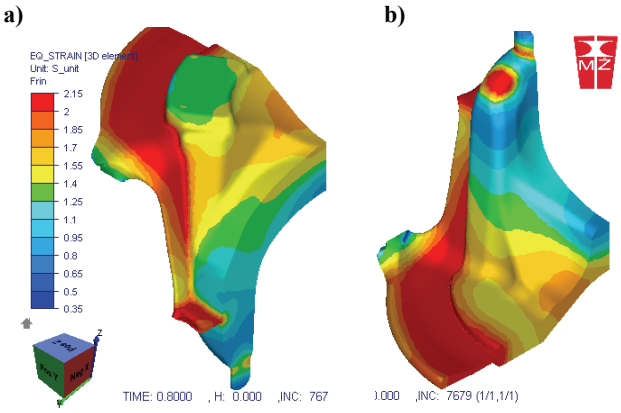

Fig. 8. *Strain distribution after second deformation.*

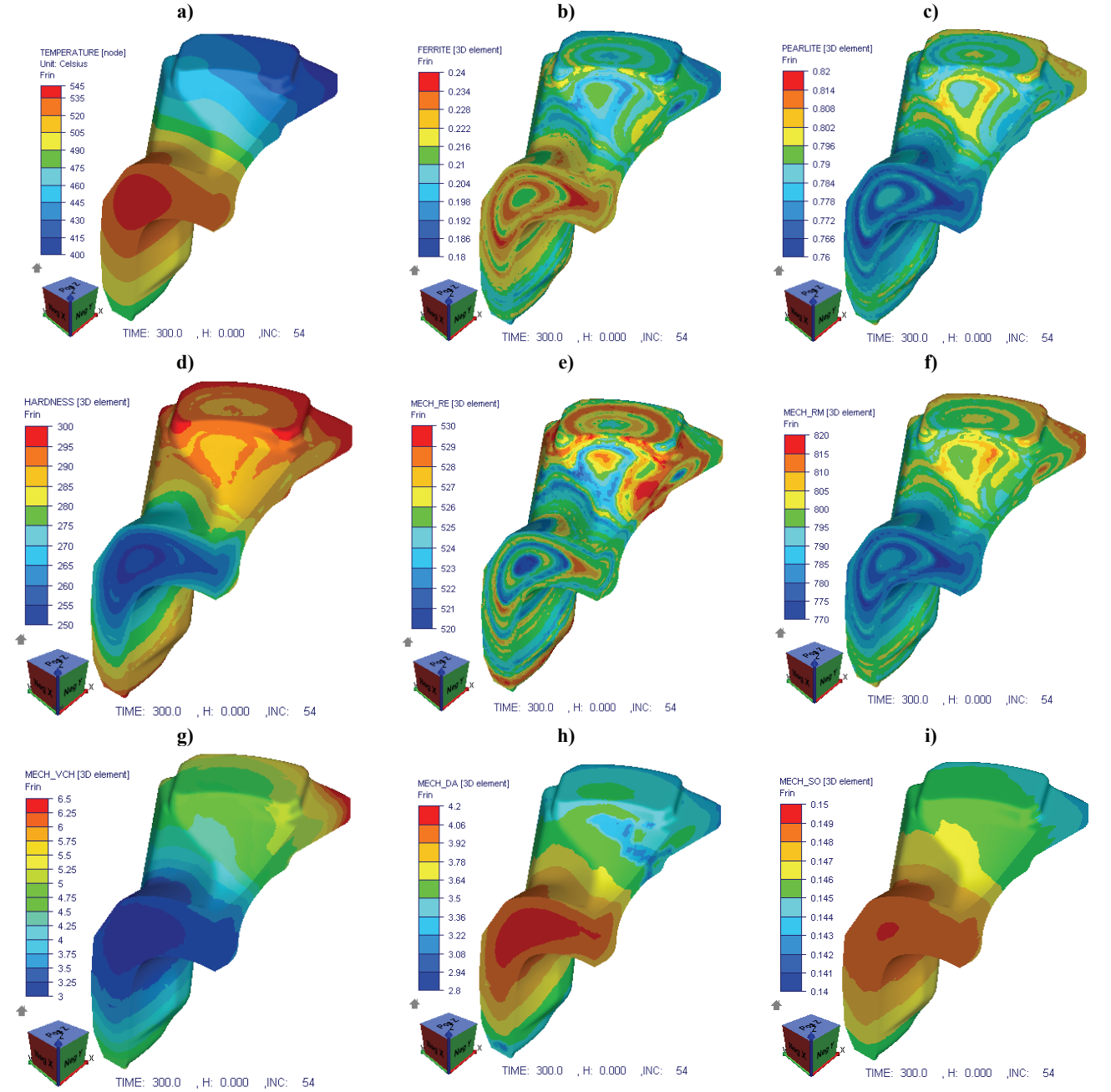

Fig. 9. *Distribution of FORGE models parameters: (a) temperature, (b) ferrite and (c) pearlite volume fraction, (d) Vickers hardness. Distribution of parameters from calculations implemented into code: (e) yield stress σ_y, (f) ultimate strengths σ_s, (g) cooling rate C_γ, (h) ferrite grain size, (i) pearlite interlamellar spacing.*

6. SUMMARY

The rheological, microstructure evolution and phase transformation model was developed to simulate the forging process and accelerated – controlled cooling of Cardan joint produced of C45 grade steel. Rheological model was built using Sellars model in which kinetic equation for dynamic recrystallization was incorporated. Also, classical equations for microstructure evolution were used to simulate dynamic, metadynamic and static recrystallization, as well as grain growth after recrystallization. Built-in Forge module was used to simulate the phase transformations during cooling. Empirical equations incorporating ferrite – pearlite microstructure parameters were used to predict yield strength and ultimate tensile strength. The model was used to investigate the effect of accelerated – controlled cooling with fans on the strength properties of Cardan joint. The results of the predictions compare fairly well with the measurements, and in the future the developed model will be used to adjust the cooling conditions to achieve required properties of forgings.

ACKNOWLEDGEMENT

The authors would like to acknowledge the financial support (PC 6 ZR7 2008 C/07018) provided for this study by the Ministry of Science and Higher Education, Poland.

REFERENCES

Davenport, S.B., Silk, N.J., Sparks, C.N., Sellars, C.M., 1999, Development of constitutive equations for the modelling of hot rolling, *Mat. Sci. Techn.*, 16, 1-8.

Kowalski, B., Sellars, C.M., Pietrzyk, M., 2000, Development of a computer code for the interpretation of results of hot plane strain compression tests, *ISIJ Int.*, 40, 1230-1236.

Kuziak, R., Cheng, Y.W., Glowacki, M., Pietrzyk, M. , 1997, *Modeling of the microstructure and mechanical properties of steels during thermomechanical processing*, NIST Technical Note, No. 1393

Kuziak, R., Pidvysots'kyy, V., Opara, J., Wrożyna, A., Molenda, R., 2010, *Przeprowadzenie symulacji numerycznej regulowanej obróbki cieplno-plastycznej i przyspieszonego chłodzenia po kuciu dla wybranych typów odkuwek dla przemysłu motoryzacyjnego*, cz. II, PC-0119-04 (in Polish, not published)

Lee, C.H., Kobayashi, S., 1973, New solution to rigid plastic deformation problems, ASME, *J. Eng. Ind.*, 95, 865-873.

Saunders, N., Guo, Z., Li, X., Miodownik, A.P., Schillé, J.-P., 2004, *The Calculation of TTT and CCT diagrams for General Steels*, Thermotech Ltd., Surrey Technology Centre, The Surrey Research Park, U.K.

Li, M.V., Niebuhr, D.V., Meekisho, L.L., Atteridge, D.G., 1998, A computational model for the prediction of steel hardenability, *Metall. Mater. Trans. B*, 29B, 661-72.

SYMULACJA PROCESÓW TERMOMECHANICZNYCH PODCZAS KUCIA NA GORĄCO I PROGNOZOWANIE WŁAŚCIWOŚCI MECHANICZNYCH ODKUWEK

Streszczenie

W artykule przedstawiono wyniki symulacji fizycznych oraz numerycznych procesów kucia i przyspieszonego-kontrolowanego chłodzenia po kuciu. Dla symulacji na podstawie eksperymentów wykonanych na urządzeniach Gleeble 3800 i DIL 805A/D opracowano model reologiczny, rozwoju mikrostruktury oraz model przemian fazowych. Wszystkie modele zostały zaimplementowane w kodzie MES. W symulacji numerycznej obliczono parametry charakteryzujące mikrostrukturę oraz właściwości mechaniczne materiału odkuwek. Wyniki symulacji porównano z danymi dla rzeczywistych odkuwek.

Received: November 3, 2010
Received in a revised form: November 26, 2010
Accepted: December 10, 2010